

Pharmaceutical Nanotechnology

## Effect of bicellar systems on skin properties

L. Barbosa-Barros<sup>a</sup>, C. Barba<sup>a</sup>, M. Cócera<sup>b</sup>, L. Coderch<sup>a</sup>,  
C. López-Iglesias<sup>c</sup>, A. de la Maza<sup>a</sup>, O. López<sup>a,\*</sup>

<sup>a</sup> *Departament de Tecnologia de Tensioactius, Institut d'Investigacions Químiques i Ambientals de Barcelona (I.I.Q.A.B.), Consell Superior d'Investigacions Científiques (C.S.I.C.), C/ Jordi Girona 18-26, 08034 Barcelona, Spain*

<sup>b</sup> *Unitat de Biofísica, Departament de Bioquímica i Biologia Molecular, Fac. Medicina UAB, Edifici M, 08193 Bellaterra (Barcelona), Spain*

<sup>c</sup> *Serveis Científicotècnics, Universitat de Barcelona, Parc Científic de Barcelona, C/ Josep Samitier 1-5, 08028 Barcelona, Spain*

Received 14 June 2007; received in revised form 12 October 2007; accepted 15 October 2007

Available online 22 October 2007

### Abstract

Bicelles are discoidal aggregates formed by a flat dimyristoyl-glycero-phosphocholine (DMPC) bilayer, stabilized by a rim of dihexanoyl-glycero-phosphocholine (DHPC) in water. Given the structure, composition and the dimensions of these aggregates around 10–50 nm diameter, their use for topical applications is a promising strategy. This work evaluates the effect of DMPC/DHPC bicelles with molar ratio (2/1) on intact skin. Biophysical properties of the skin, such as transepidermal water loss (TEWL), elasticity, skin capacitance and irritation were measured in healthy skin *in vivo*. To study the effect of the bicellar systems on the microstructure of the stratum corneum (SC) *in vitro*, pieces of native tissue were treated with the aforementioned bicellar system and evaluated by freeze substitution applied to transmission electron microscopy (FSTEM). Our results show that bicelles increase the TEWL, the skin elastic parameters and, decrease skin hydration without promoting local signs of irritation and without affecting the SC lipid microstructure. Thus, a permeabilizing effect of bicelles on the skin takes place possibly due to the changes in the phase behaviour of the SC lipids by effect of phospholipids from bicelles.

© 2007 Elsevier B.V. All rights reserved.

**Keywords:** Freeze-substitution transmission electron microscopy; Tewl; Skin hydration; Biophysical properties of skin; Stratum corneum permeability; Stratum corneum microstructure

### 1. Introduction

Bicelles are discoidal aggregates constituted by a flat dimyristoyl-glycero-phosphocholine (DMPC) bilayer, stabilized by a rim of dihexanoyl-glycero-phosphocholine (DHPC) in water (Fig. 1) (Sanders and Landis, 1995; Triba et al., 2005). The size of these structures is controlled by the molar ratio of the long/short-chain phospholipid ( $q$ ) and the total phospholipid concentration (cL). This system was developed to solve experimental problems of current membrane models in NMR studies of protein characterization, such as low reorientation rates and high phospholipid packing curvature (Vold et al., 1997). Nowadays, the use of bicelles is mainly based on their ability to spon-

aneously align in magnetic fields (Marcotte and Auge, 2005; Triba et al., 2005). Due to the presence of a planar core region, bicelles mimic sections of natural membranes. This fact allows to orient membrane proteins inserted in the bilayer structure and to study the superficial interactions between proteins and the phospholipid bilayer (Whiles et al., 2002).

The bilayered structure and dimensions of bicelles, with diameters in the range of 10–50 nm and thickness about 4–6 nm, are slightly different from those of liposomes and micelles. These two nanostructures have often been used for skin treatment (Muller-Goymann, 2004; Elsayed et al., 2007) although their application is debated due to some aspects. Liposomes are too large to penetrate into the narrow intercellular spaces of stratum corneum (SC) (Benson, 2005). Concerning the micelles, the usual presence of surfactant in their composition supposes a problem due to the well known irritating effect of these solubilising agents on the skin (Kartono and Maibach, 2006). In this line, the use of bicelles for skin treatment may report advantages comparing to the use of liposomes and micelles: the size of bicelles is

*Abbreviations:* Cer, ceramide; DHPC, dihexanoylphosphocholine; DMPC, dimyristoylphosphocholine; FSTEM, freeze-substitution transmission electron microscopy; SC, stratum corneum; TEWL, trans epidermal water loss.

\* Corresponding author. Tel.: +34 93400 61 00; fax: +34 93204 59 04.

E-mail address: [oloesi@cid.csic.es](mailto:oloesi@cid.csic.es) (O. López).

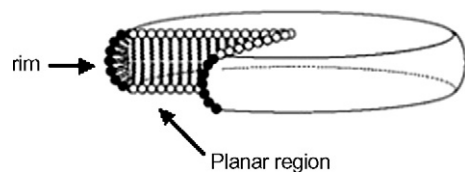


Fig. 1. Schematic representation of a bicelle showing the planar region, composed of long-chain phospholipid, surrounded by a rim of short-chain phospholipid.

small enough for passing through the SC lipid lamellae and their composition consists exclusively of lipids. These features open new possibilities of applications for this innovative system in skin research. Due to its bilayered structure, bicelles can be useful as drug carriers through the skin. In addition, these structures potentially represent a new model for skin lipids studies.

In earlier works we have studied the structure and composition of the SC (Coderch et al., 2002; López et al., 2001, 2007) as well as the effect of different nanostructures and molecules, such as liposomes with varying compositions, lipid mixtures, surfactants, organic solvents, etc., on the skin, particularly on the SC (López et al., 2000a,b, 2002). We have demonstrated the disturbing effect of surfactants on SC microstructure and on skin conditions and, inversely, the beneficial effect of structures containing lipids similar to those present in SC. In the present work, the effect of bicelles on the SC microstructure and on the skin biophysical properties is investigated for the first time. Bicellar systems combine the necessary requirements for skin applications. Since phospholipids may increase the water content of skin (Betz et al., 2005) the parameters skin hydration and elasticity were chosen to estimate the extent of penetration of the bicelles into skin. Erythema measurements were used to indicate the skin tolerance to the bicelles and, transepidermal water loss (TEWL) reported on the barrier integrity (Van der Geest et al., 1996). Additionally, freeze-substitution transmission electron microscopy (FSTEM) was used to evaluate *in vitro* the microstructural alterations of SC induced by bicelles.

## 2. Materials and methods

### 2.1. Chemicals

Bicelles were formed by 1,2-dimyristoyl-sn-glycero-3-phosphocholine (DMPC) and 1,2-dihexanoyl-sn-glycero-3-phosphocholine (DHPC) purchased from Avanti Polar Lipids (Alabaster, AL). The  $^{31}\text{P}$  NMR study of bicellar systems required deuterium oxide as internal standard, which was acquired from Sigma (St. Louis, MO).

Trypsin and phosphate buffered solution (PBS), needed for SC isolation, were purchased from Sigma Co. The chemicals for preparing microscopy samples were: ruthenium tetroxide ( $\text{RuO}_4$ ), lowicryl HM20, glutaraldehyde and cacodylate buffer which were supplied by Electron Microscopy Sciences (Hatfield, PA, USA), methanol and potassium ferrocyanide ( $\text{K}_4\text{Fe}(\text{CN})_6$ ) provided by Merck, and osmium tetroxide ( $\text{OsO}_4$ ) purchased from Pelco International, Redding CA, USA.

### 2.2. Preparation and characterization of the bicellar system

Taking into account the objective of using bicelles for skin penetration, the molar ratio  $q=2$  was chosen to obtain small aggregates. This molar ratio was previously described for structures with about 20 nm of diameter (Marcotte and Auge, 2005). Samples were prepared by mixing appropriate amounts of DMPC powder and a DHPC chloroform solution to reach DMPC/DHPC molar ratio,  $q=2$ . After mixing the components, the chloroform was removed with a rotary evaporator and the systems were hydrated with water to reach 20% (w/v) of total lipid concentration. The sample for  $^{31}\text{P}$  NMR was hydrated with deuterium oxide instead of water. Bicellar solutions were prepared by subjecting the sample to several cycles of sonication and freezing until sample became transparent (Triba et al., 2005). The systems were analysed 24 h and 14 days after preparation by  $^{31}\text{P}$  nuclear magnetic resonance ( $^{31}\text{P}$  NMR), small angle X-ray scattering (SAXS) and dynamic light scattering (DLS). Additionally, they were visualized by freeze-fracture electron microscopy (FFEM) in order to characterize the morphology of the aggregates. Samples were maintained under refrigeration ( $\approx 4^\circ\text{C}$ ) during the 14 days of experiment and the measurements were performed at room temperature.

#### 2.2.1. $^{31}\text{P}$ -NMR

The NMR spectra were recorded on a Varian System 400 MHz spectrometer equipped with a 5 mm probe at room temperature.  $^{31}\text{P}$ -NMR spectra were recorded at 161.901 MHz using a single pulse, quadrature detection, complete phase cycling of the pulses, and proton decoupling during the signal acquisition. Typical acquisition parameters are as follows: pulse length of 8.5  $\mu\text{s}$ , recycle delay of 0.5 s, spectral width of 6868.1 Hz, and 22 K data size. Spectra were referenced to 85% phosphoric acid.

#### 2.2.2. Small angle X-ray scattering

SAXS measurements were carried out using a Kratky camera of small angle (M Braun) coupled to a Siemens KF 760 (3 KW) generator. Nickel-filtered radiation with wavelength corresponding with the Cu  $\text{K}\alpha$  line (1.542 Å) was used. The linear detector was PSD-OED 50 M-Braun, and the temperature controller was a Peltier KPR AP PAAR model. The sample was inserted between two Mylar sheets with a 1 mm separation. The SAXS curves were smoothed by fitting a degree three polynomial to an increasing number of points as the channel number increases. The fitting software has been designed to guarantee constant slopes and fixed peak position. The system uses a line collimated beam, therefore, to preserve sharpness, the smoothed curves were desmeared using the procedure of Singh (Singh et al., 1993). The SAXS curves are shown as a function of the scattering vector modulus

$$q = \frac{4\pi}{\lambda} \sin \theta \quad (1)$$

where  $\theta$  is the scattering angle and  $\lambda$  the wavelength of the radiation (1.542 Å). The position of the diffraction peaks are directly related to the repeat distance of the molecular structure,

as described by Bragg's law

$$2d \sin \theta = n\lambda \quad (2)$$

in which  $n$  and  $d$  are the order of the diffraction peak and the repeat distance, respectively. In the case of a lamellar structure, the various peaks are located at equidistant positions, then

$$qn = \frac{2\pi n}{d} \quad (3)$$

being  $qn$  the position of the  $n$ th order reflection.

### 2.2.3. Dynamic light scattering

The hydrodynamic diameter (HD) and polydispersity index (PI) were determined by means of DLS using a Zetasizer Nano ZS (Malvern Systems, Southborough, MA). The DLS measures the Brownian motion of the particles and correlates this to the particle sizes. The relationship between the size of a particle and its speed due to Brownian motion is defined in the Stokes–Einstein equation:

$$\text{HD} = \frac{kT}{3\pi\eta D} \quad (4)$$

where HD is the hydrodynamic diameter,  $D$  is the translational diffusion coefficient ( $\text{m}^2/\text{s}$ ),  $k$  is the Boltzmann's constant ( $1.3806503 \times 10^{-23} \text{ m}^2 \text{ kg s}^{-2} \text{ K}^{-1}$ ),  $T$  is the absolute temperature (K) and  $\eta$  is the viscosity ( $\text{mPa s}$ ).

### 2.2.4. Freeze-fracture electron microscopy

FFEM study was carried out according to the procedure described by Egelhaaf (Egelhaaf et al., 1996). About  $1 \mu\text{L}$  of suspension was sandwiched between two copper platelets using 400-mesh gold grids as spacer. Then the sample was frozen by plunging in propane at  $-180^\circ\text{C}$  and fractured at  $-150^\circ\text{C}$  and  $2 \times 10^{-7}$  mbar in a Balzers BAF 300 freeze-fracturing apparatus (BAL-TEC, Liechtenstein). The replicas were obtained by unidirectional shadowing with 2 nm of Pt/C and 20 nm of C, and they were floated on distilled water and examined in a JEOL 1010 TEM electron microscopy at 80 kV.

## 2.3. In vitro study

### 2.3.1. Stratum corneum isolation

Sections of human fresh skin excised for clinical reasons in the Department of Dermatology, University Hospital "Principes de España", Barcelona, Spain, were placed in water at  $65^\circ\text{C}$  for 4–5 min, and the epidermis was scraped off in sheets. These sheets were placed in 100 ml of 0.5% trypsin in PBS (pH 7.4,  $4^\circ\text{C}$ , overnight). The SC pieces were then collected, rinsed in distilled water, and suspended in a large volume of water. The pieces were transferred to a round flask with fresh trypsin/PBS solution and rotated at 100 rpm ( $25^\circ\text{C}$ , 2 h). Then, the SC pieces were washed with distilled water (López et al., 2007) and incubated separately with bicelles and deionised water for 18 h at room temperature.

### 2.3.2. FSTEM experiments

The SC was cut into small ribbons with a size of approximately  $2 \text{ mm} \times 1 \text{ mm}$ . The ribbons were fixed in 5% (w/v) glutaraldehyde in 0.1 M sodium cacodylate buffer, pH 7.2, and postfixed in 0.2% (w/v)  $\text{RuO}_4$  in sodium cacodylate buffer, pH 6.8 with 0.25% (w/v) potassium ferrocyanide ( $\text{K}_4\text{Fe}(\text{CN})_6$ ). After 1 h, the  $\text{RuO}_4$  solution was replaced by fresh  $\text{RuO}_4$  in order to establish an optimal fixation. After rinsing in buffer, the tissue samples were cryofixed by rapid freezing on a liquid nitrogen-cooled metal mirror (Cryovacublock, Leica) at  $-196^\circ\text{C}$  prior to freeze substitution.

The freeze-substitution procedure was carried out in an AFS (Automatic Freeze Substitution) system (Leica). The tissue samples were cryosubstituted at  $-90^\circ\text{C}$  for 48 h using 100% methanol, containing 1.0% (w/v) osmium tetroxide ( $\text{OsO}_4$ ), 0.5% (w/v) uranyl acetate and 3.0% (w/v) glutaraldehyde. After the 48 h substitution period, the temperature was raised to  $-50^\circ\text{C}$ , the samples were washed 3 times in 100% methanol, and subsequently the methanol solution was gradually replaced by the embedding medium Lowicryl HM20 (100%). This resin was replaced after 24 and 48 h by freshly made embedding medium. Finally the samples were transferred to a mould containing Lowicryl, and were incubated for 48 h at  $-50^\circ\text{C}$  under UVA-radiation, to allow polymerisation. Ultrathin sections were cut (Ultracut UCT, Leica), transferred to formvar-coated grids and examined in a Hitachi 600 transmission electron microscope. For each sample, 10 overviews and approximately 30–40 detail electron micrograph were taken (Van den Bergh et al., 1999; López et al., 2002).

## 2.4. In vivo study

### 2.4.1. Study design

Non-invasive biophysical parameters were measured in order to evaluate the effect of bicelles on the *in vivo* skin. Intra-individual comparison of three test areas on the volar forearm of volunteers was carried out. Bicelles, deionised water and control (non-treated) areas were randomized to the test sites on each subject. Considering that bicelles had been prepared with 80% water content, deionised water was applied in one of the test areas to observe the isolated effect of this substance.  $10 \mu\text{L}$  of sample 20% (w/w) and of deionised water were applied daily over a period of 10 days on 6 healthy caucasian females (age 25–38) with no visible skin abnormalities. The subjects were not allowed to use moisturizers on the lower arm for one week prior to, and during the days of the experiments. The volunteers were accommodated in an air-conditioned room at  $21 \pm 1^\circ\text{C}$  and  $50 \pm 5\%$  relative humidity for 15 min before the measurements were carried out. The skin properties were measured prior to the application of bicelles, on day 0. From then, measurements were carried out daily, 24 h after sample application until 1 day after the last application (day 11). In order to be able to make valuable statements on the effect of the bicellar system, the results were calculated with the following equation (Yilmaz and Borchert, 2006):

$$\text{changes in skin property (\%)} = \frac{Q_{tv}}{(Q_{0v} - 1)} \times 100 \quad (5)$$

where,  $Q_{tv}$  is the mean of the quotients of the measured values of treated and untreated skin area after application time  $t$  of all volunteers  $v$ , and  $Q_{0v}$  is the mean of quotients of the measured values of treated and untreated skin area before application time of all volunteers.

#### 2.4.2. Transepidermal water loss

The measurement of water evaporation rates with the Tewameter TM 300 (Courage and Khazaka, Electronic GmbH, Cologne, Germany) is based upon diffusion principles in an open cylinder system  $dm/dt = -DA dp/dx$  (where  $A$  represents the surface in  $m^2$ ,  $m$  the water transported in g,  $t$  the time in h,  $D$  the diffusion constant  $0.877 \text{ g/m h}$ ,  $p$  the vapour pressure of the atmosphere in mmHg and  $x$  the distance from the skin surface to the point of measurement in m) according to Fick's law (Miteva et al., 2006). Measurement values are given in  $\text{g/m}^2 \text{ h}$ .

#### 2.4.3. Skin hydration

The experiment of the skin humidity was carried out with a Corneometer 825, which was mounted on a Multi Probe Adapter MPA5 (Courage and Khazaka, Electronic GmbH, Cologne, Germany). The measurement is based in the capacitance method that uses the relatively high dielectric constant of water compared to the substances of the skin. Three measurements were performed in each testing area at different points of the volar forearms.

#### 2.4.4. Skin elasticity

The measurement of the elastic parameters were performed using a Cutometer SEM 575 (Courage and Khazaka Electronic GmbH, Cologne, Germany) based on a suction- and elongation method. The cutometer exhibited deformation-time curves from which the following parameters were calculated:  $U_f$ ,  $U_r/U_e$  and  $U_r/U_f$ .  $U_f$  is the maximal skin extension and it is associated with skin distensibility.  $U_e$  represents the elastic deformation or immediate extensibility and  $U_r$  corresponds to the elastic immediate recovery or tonicity. The relative parameter  $U_r/U_e$  reflects the net elasticity of the skin without viscous deformation and the  $U_r/U_f$  represents the biological elasticity, i.e. the ratio of immediate retraction to total extension. Absolute parameters are influenced by skin thickness, whereas relative parameters are not and, thus, can be compared without preliminary standardization to skin thickness (Seok Yoon et al., 2002; Holzer et al., 2005; Bazin and Fanchon, 2006).

#### 2.4.5. Erythema and skin irritation

Ocular inspection of the test areas were daily performed and any kind of change in skin surface was recorded. The pathological parameter erythema, was measured photometrically by a Mexameter 18 (Courage and Khazaka Electronic GmbH, Cologne, Germany) based on remission principle. A receiver measures the light reflected by the skin. The erythema index

was calculated by the instrument according to the equation:

$$EI = \left( \frac{500}{\log 5} \right) \left( \log \left( \frac{\text{red-reflection}}{\text{green-reflection}} \right) + \log 5 \right) \quad (6)$$

Each measurement was performed in triplicate on different points of the volar forearms.

#### 2.4.6. Data treatment

The mean values and standard deviations (S.D.) were calculated and presented in column graphics with error bars. The results were doubly evaluated as a percentage of modification respect to the basal (initial value) and control zones. The mean of the initial values of skin before treatment is represented in the "y" axis of the graphics as the 100% value.

The Dixon's test was used for detecting outliers, which were excluded from the data. The ANOVA variance analysis was used to determine significant differences between values obtained from different treatments (significance level accepted,  $*p < 0.05$ ) using the Statgraphics® program.

### 3. Results

#### 3.1. Evaluation of the bicellar system: $^{31}\text{P}$ NMR, SAXS, DLS and FFEM

Fig. 2 shows the  $^{31}\text{P}$  NMR spectra for DMPC/DHPC bicelles 24 h (2A) and 14 days (2B) after preparation. A doublet is observed with peaks around  $-0.754$  and  $-0.927$  ppm (2A) and  $-0.764$  and  $-0.935$  ppm (2B), in addition to the reference peak sited at  $0.000$  ppm. This spectral appearance was previously reported by others authors for small disks in rapid rotation (Tribat et al., 2005). The reproducibility of the bicelles characteristic resonances in the spectrum of 24 h and 14 days (Fig. 2A and B) indicates good structural stability of the sample for at least 2 weeks. Fig. 3 plots the SAXS curve of bicelles 24 h after preparation. No difference was detected between this scattering curve and the one corresponding to 14 days after preparation (data not shown). This fact also corroborates the stability of the system. The lamellar repeated distance  $d$  was estimated from the analysis of the peak by the Bragg's law and was attributed to the bilayer thickness in a similar way that studies with liposomes and other bilayer models (Singh et al., 1993). A repeat distance value of  $d = 4.5 \text{ nm}$  was obtained in both spectra (24 h and 14 days after preparation) suggesting that no alteration in the bilayer occurred during the 14 days of experiment. The size distributions curves obtained by DLS exhibited a monomodal distribution with a HD of  $15.9 \text{ nm}$  and PI of  $0.211$ , 24 h after preparation. Values for the same sample 14 days after preparation resulted very similar: HD =  $16.3 \text{ nm}$  and PI =  $0.303$ . The HD obtained by DLS is that of a hypothetical hard sphere that diffuses with the same speed as the particle under experiment. As the bicelles present a flat appearance, the values of particle size obtained with this technique can be considered as an estimation of the structure's dimension. The particle size values obtained by this technique show quite good agreement with the structure sizes visualized by FFEM (Fig. 4). The micrograph shows structures with sizes around  $20 \text{ nm}$  in which a discoidal shape



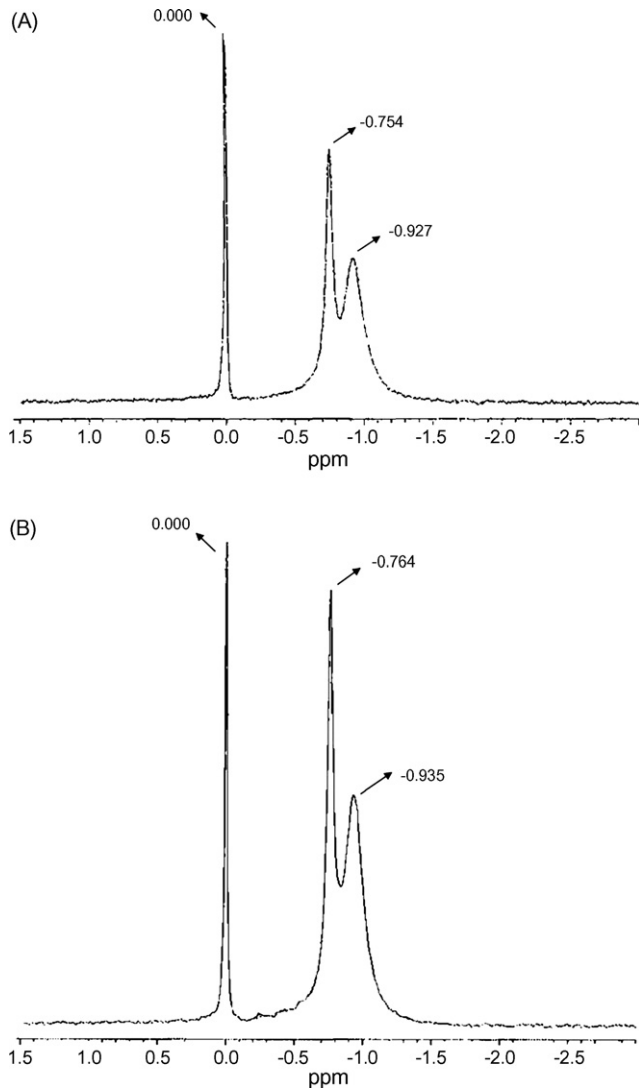


Fig. 2.  $^{31}\text{P}$  NMR spectra for DMPC/DHPC bicelles 24 h (A) and 14 days (B) after preparation.

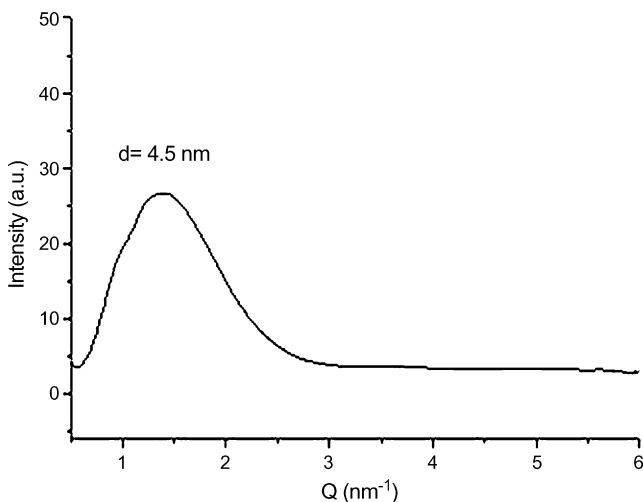


Fig. 3. Small angle X-ray scattering (SAXS) curve of bicelles 24 h after preparation.

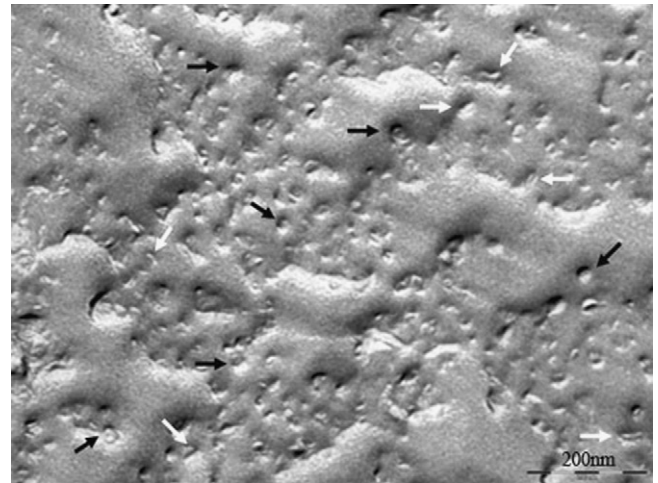


Fig. 4. FFEM micrograph of DMPC/DHPC  $q=2$  bicelles. The image depicts a zone full of bicelles. Black arrows denote disks viewed face-on and white arrows denote disks viewed edge-on.

is observed. Face (black arrows) and the edges (white arrows) areas are clearly visualized. Similar structures were reported by other authors using other electron microscopy techniques (Glover et al., 2001; Arnold et al., 2002; van Dam et al., 2004, 2006).

In resume, the physicochemical characterization of the bicellar system indicates structural stability at least for 14 days after preparation, which guarantees the integrity of the samples during the *in vivo* experiment.

### 3.2. Structure of native and treated SC with DMPC/DHPC bicelles: FSTEM

FSTEM allow us to accurately visualize the SC tissue. Fig. 5 shows native SC, previously to the treatment with the bicellar system. The pictures show that  $\text{RuO}_4$  fixation is limited to a maximum of 6–10 cell layers from the skin surface downwards. Therefore, some skin bilayers in lower parts of the SC cannot be visualized and consequently intercellular spaces appear as “empty”. Fig. 5A and B clearly show skin corneocytes (C), flattened cells characterized by the absence of cell organelles and the presence of electron dense keratin filaments. In the intercellular spaces, lipid bilayers (L) and corneosomes (CD) (SC desmosomes representing contact areas between adjacent corneocytes) are visualized. In Fig. 5A, an overview of the SC is shown, whereas Fig. 5B depicts an enhanced micrograph of the intercellular lipids (L) and corneosomes (CD) from native SC. Micrograph from Fig. 6 show low (A) and high (B) magnifications of SC sections after treatment with bicelles. In a similar way that native sample, the SC treated with bicelles showed corneocytes, corneosomes and, in the intercellular spaces, the lipid lamellae were also clearly visualized. No microstructural differences were visualized on SC treated with bicelles in comparison to the non-treated SC. These findings indicate that no apparent damage was produced on the SC microstructure by the effect of bicelles.

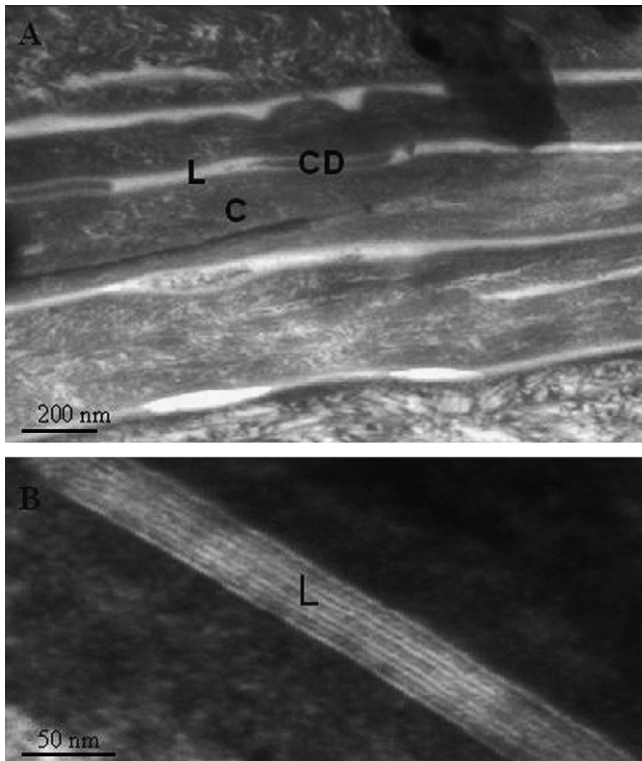


Fig. 5. FSTEM micrograph of native SC. Picture A: overview. Picture B: enhanced area in which lamellar structure is visualized. Symbols: corneocytes (C), lipids (L) and corneodesmosomes (CD).

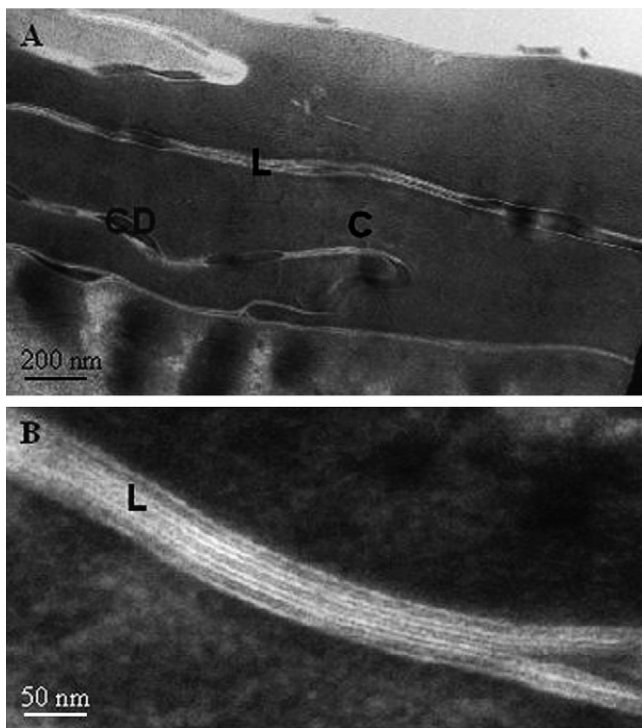


Fig. 6. FSTEM micrograph of SC after incubation with bicelles. Picture A: overview. Picture B: enhanced area in which lamellar structure is visualized. Symbols: corneocytes (C), lipids (L) and corneodesmosomes (CD).

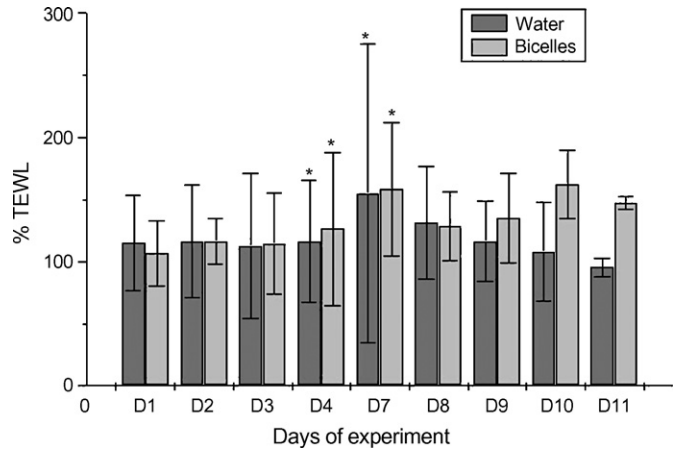


Fig. 7. Variation of relative TEWL values during the treatment period for control and treated areas. Changes were doubly evaluated versus basal and control values. (\* $p < 0.05$ , significance is evaluated using ANOVA variance analyses between each percentage results and their corresponding control percentage results.)

3.3. In vivo experiments: biophysical measurements

Fig. 7 shows that consecutive application of bicelles on the skin promotes an increase of 47.2% in TEWL from days 0 to 11. The average values evolve sequentially after every measurement, except at day 7, in which a considerably increase of values is observed. Taking into account that the peak for the water zone in this specific day also increased in similar amplitude, we can consider this event as external from the experiment, possibly instrumental or environmental-related. In our experiment the maximum TEWL absolute value was 17 g/m<sup>2</sup>/h (only detected for one of the volunteers in the last day of measurement) and the means in whatever case were always below 10 g/m<sup>2</sup>/h. TEWL values associated to damaged skin of volar forearm have been described in the range of 25–40 g/m<sup>2</sup>/h (Branco et al., 2005; Kim et al., 2006). Hence, although the experiment indicates that application of bicelles on SC induces an increase

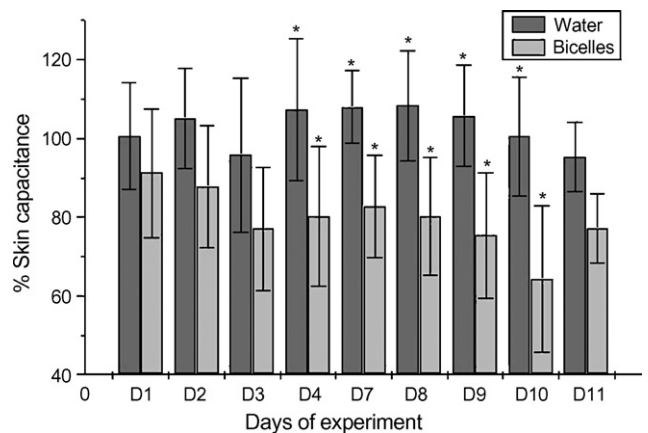


Fig. 8. Changes in the skin hydration measured as relative variations in the electrical capacitance during the treatment period for control and treated areas. Changes were doubly evaluated versus basal and control values. (\* $p < 0.05$ , significance is evaluated using ANOVA variance analysis between each percentage results and their corresponding control percentage results.)

Table 1

Mean absolute values and standard deviation (S.D.) corresponding to the elastic biomechanical parameters  $U_f$ ,  $U_r/U_e$  and  $U_r/U_f$  before (day 1) and after (day 11) treatment in test area (treated with bicelles) and control areas (non-treated area)

	Test areas				Control areas			
	Day 1		Day 11		Day 1		Day 11	
	Mean	S.D.	Mean	S.D.	Mean	S.D.	Mean	S.D.
$U_f$	0.240	0.03	0.230	0.04	0.270	0.06	0.260	0.03
$U_r/U_e$	0.805	0.33	0.842	0.08	1.002	0.14	0.908	0.22
$U_r/U_f$	0.637	0.18	0.664	0.03	0.734	0.13	0.677	0.17

S.D.: standard deviation.

of the TEWL, the values detected never reached pathological levels.

Changes in the skin hydration measured as variations in the electrical capacitance are plotted in Fig. 8. It is shown that application of bicelles decreased sequentially the skin capacitance. A pronounced fluctuation at day 10, i.e. after the 7th of application is observed. The skin capacitance decreases to be further recovered at day 11. Since data obtained for the water zone did not show the same tendency, this fluctuation could be related to some inter-individual variation. The initial (before the first application) mean value of capacitance was 35.4 a.u., and the mean value in the last day of experiment was 26.07 a.u. indicating a decrease about 26% of this parameter by effect of bicelles treatment.

Biomechanical parameters  $U_f$ ,  $U_r/U_e$  and  $U_r/U_f$  were also measured. The relative percentages of these parameters showed slight differences between the areas treated with bicelles and the control areas. Table 1 shows the mean absolute values and the standard deviation (S.D.) obtained before (day 1) and after treatment (day 11) in test area (treated with bicelles) and in control areas (non-treated areas). It is shown that values of  $U_f$  decreases from 0.24 (before bicelle treatment) to 0.23 (after bicelle treatment). However, this decrease is not significant given that control areas also indicated a decrease from 0.27 to 0.26 during the

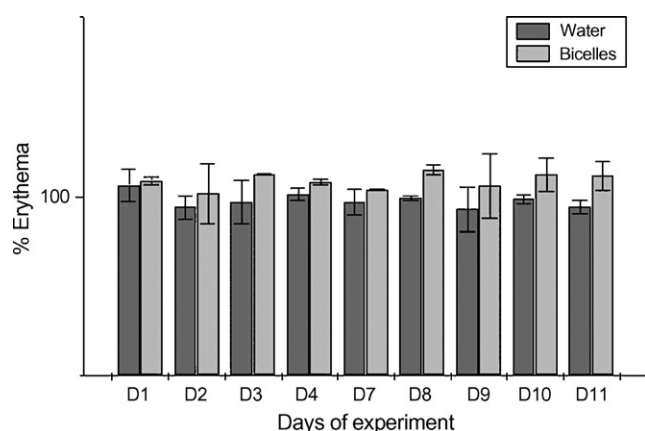


Fig. 9. Variation of relative erythema index values during the treatment period for control and treated areas. Changes were doubly evaluated versus basal and control values. (\* $p < 0.05$ , significance is evaluated using ANOVA variance analyses between each percentage results and their corresponding control percentage results).

same period. A slight increase of  $U_r/U_e$  and  $U_r/U_f$  parameters in areas treated with bicelles is also observed. Interestingly, control areas show decrease in these parameters indicating that values obtained for test areas could be even more pronounced.

Ocular inspections of the treated areas did not report any irritant effect of bicelles and no volunteer perceived irritation or annoyances in the test zones. Additionally, the erythema index was evaluated photometrically using the Mexameter. The percentage changes in the erythema considering inter- and intra-individual variability in areas treated with bicelles or with water are plotted on Fig. 9. The maximum change in this parameter was detected on day 8 and resulted on an increase of 1.5% which is not indicative of an irritation process (Holm et al., 2006). Besides, this percentage decreased in the following days of treatment with bicelles. Thus, the results report no evidence for any irritant effect of bicellar systems on the skin.

#### 4. Discussion

Bicellar systems formed with high DHPC proportions (typically  $q \leq 2.5$ ) have been described as small isotropic disks (Whiles et al., 2002). In these systems the DMPC is organized as a flat bilayer while the DHPC is mainly located in the edges of the structures (Triba et al., 2005). The typical  $^{31}\text{P}$  NMR spectrum of systems with these characteristics is composed by a low field doublet near  $-1.000$  ppm (Marcotte and Auge, 2005), which reflects slightly different environments of the DMPC and DHPC on the bicelle structure. Our spectra (Fig. 2A and B) accurately reproduce this description indicating the presence of small bicelle disks in the sample solution. In addition, SAXS and DLS experiments reported dimensions for these disks (16 nm diameter and 4.5 nm thickness, approximately) that are consistent with the FFEM micrograph and with the data published by other authors (Vold and Prosser, 1996). The shape of broad maximum in the SAXS curves is similar to that observed for unilamellar liposomes (Bouwstra et al., 1993), suggesting the non-stacking organization of bicelles, as it could be expected from an isotropic discoidal system. Besides, the d-spacing value 4.5 nm, associated to bilayer thickness, is in accordance with results from Kucerda, obtained with DMPC vesicles (Kucerka et al., 2004).

Considering the structure of SC, corneocytes embedded on a lipid matrix formed by lipid lamellae with very narrow interlamellar spaces (Coderch et al., 2002), the pass of small bicelles through the lipid region seems reasonable. This fact is interesting given that other lipid vehicles used for topical applications have bigger dimensions and, such a thing difficult their pass through the SC (Benson, 2005). Thus, taking into account the structural data obtained with the above mentioned techniques, the bicellar system used in this study has the appropriate size to reach internal structures of this tissue. In spite of this possibility, FSTEM images from SC before and after incubation with bicelles did not show differences, which seems to indicate that bicelles could interact with SC lipids apparently without promoting microstructural modifications.



Given that experimental conditions *in vivo* and *in vitro* are different, the comparison of the effect of bicelles on skin parameters *in vivo* with the microstructural events observed *in vitro* has to be done carefully. The *in vivo* experiment was organized sequentially and the effects were observed after a protocol of consecutive applications. On the other hand, the *in vitro* experiment of microscopy was based on an intensive treatment designed for maximize the possible effect of bicelles on the microstructure, for this reason the treatment consisted in an overnight (18 h) incubation. The SC area examined by microscopy consists of a tiny section that probably do not accurately represent inter- and intra-variability of the whole skin *in vivo*. However, no apparent modification in the SC lipid structure was observed after the intensive incubation with bicelles. This fact allows us to assume with certain reliability the preservation of the lipid structure of the *in vivo* treated skin. The skin irritation experiment corroborates this affirmation by reporting no irritating effect of bicelles on the skin. Thus, the modifications observed on skin parameters in the volunteers by treatment with bicelles are probably not related to a microstructural damage on the SC.

The incorporation of the phospholipids from bicelles into SC lipid lamellae could induce the transition of the lipid lamellar structures of the skin from gel state to liquid crystalline, promoting increase in skin permeability and consequent increase in the TEWL. This argument is understood considering the transition temperature ( $T_m$ ) of SC lipids, about 37 °C (Gay et al., 1994), and that for phospholipids forming bicelles, about 23 °C (Koon and Blanchard, 2006). At this regard, bicelles could have similar effect as penetration enhancers such as azone and oleic acid, which cause phase transformations in the lipid domains that may be relevant in the context of skin permeation (El Maghraby et al., 2005). In comparison to these enhancers, bicelles would have the additional advantage of not promoting signs of skin irritation (Kanikkannan and Singh, 2002). Another explanation for the increase of the TEWL could be a possible DHPC surfactant-like effect. The DHPC is a short-chain phospholipid that forms micelles in water. Due to these characteristics, the DHPC can be mixed with phospholipid bilayers forming bicelles. Similar effect could be produced on the SC lipids. DHPC would be incorporated in the lipid matrix giving rise to structural modifications in the lipid bilayers promoting alterations on the evaporation rates.

From the literature and our own experience many factors are known to influence *in vivo* skin biophysical parameters. These factors are either instrument related, environmental related or individual related (Pinnagoda et al., 1990). Among these factors the high inter-individual variations seen in the measured values of untreated skin play an important role (Pinnagoda et al., 1989). Due to these high inter-individual variations, comparisons between absolute values measured on different test subjects are highly problematic. Therefore we decided to compare mainly percentage changes in the skin parameters. Nevertheless, mean of absolute values allows estimating the extension of the effects of bicelles in some cases and, for this reason these values are also discussed.

TEWL is a well-established method for characterizing the integrity of the skin barrier function. Our results showed an increase in TEWL after treatment with bicelles that is often indicative of the disturbance of this protective barrier. However, given that absolute TEWL values remained hardly below those reported for impaired skin, the damage in the barrier function by effect of bicelles was discarded. Given that TEWL is a measurement of the rate of water lost through the skin, determination of this parameter is also useful to estimate the ability of the skin to retain moisture. Thus, in some cases, the increase of TEWL correlates with the decrease of water content of the skin. This fact would explain the reduced capacitance values detected in our results when TEWL increases. Diminishing hydration and water content are usually related with lost of skin elasticity and risks of cracking. It is noteworthy, however, that these consequences on the elastic properties were not observed after treatment with bicelles. In fact, elasticity measurements showed a slight improvement of the net and biological elasticity of the skin. Explanation of this lack of correlation could be that the corneometer registers the electrical capacitance of the skin surface and depicts changes of hydration to a depth of 0.1 mm (Kim et al., 2002). It is reasonable to assume that deeper layers retain water enough to preserve the elastic skin behaviour. Regarding these elasticity parameters,  $U_f$  gives information about firmness of the skin and  $U_r/U_e$  and  $U_r/U_f$  stand for the net and biological elasticity, respectively (Wissing and Müller, 2003). It is necessary to consider that the skin is 100% elastic when  $U_r/U_e$  and  $U_r/U_f$  are close to 1 (Wissing and Müller, 2003). This fact indicates that the skin recovers completely after deformation, specifically when  $U_r/U_f = 1$ . In this sense the increase in the  $U_r/U_e$  and  $U_r/U_f$  values obtained in our experiments indicates that treatment with bicelles positively affected this skin property. The high values detected for these parameters even before treatment with bicelles are indicative that volunteers had high initial skin elasticity. Due to the fact that they were  $27 \pm 4$  years old, they did not have the so-called “aged” skin.

## 5. Conclusion

Non-invasive biophysical methods increasingly gain in importance in order to prove the efficacy and safety of new systems for topical application. In the present work, some of these methods were used to evaluate the effect of bicellar systems on skin properties. Our results indicate that bicelles formed by DMPC/DHPC at  $q = 2$  and total lipid concentration  $cL = 20\%$  increase skin permeation, elastic parameters, and decrease skin hydration without affecting SC lipid microstructure and without promoting erythema or visual signs of irritation. This increase in the permeability could be related with an alteration in the phase behaviour of SC lipids by effect of phospholipids from bicelles. All in all, bicelles should be considered as new nanostructures with promising applications as drug carriers through the skin. These systems could have an enhancer effect on skin permeability and could incorporate different compounds in their lipid structure, questions that should be investigated in future works.



## Acknowledgements

The authors would like to thank Pedro González from Transtechnics S.L. for providing technical and financial support for this project. We acknowledge Dr. Ana Linares for her expert assistance on the NMR experiments and to Sonia Ruíz and Elisenda Casals for helping in TEM. We are also indebted to the volunteers who participated in this trial.

## References

- Arnold, A., Labrot, T., Oda, R., Dufourc, E.J., 2002. Cation modulation of bicelle size and magnetic alignment as revealed by solid-state NMR and electron microscopy. *Biophys. J.* 83, 2667–2680.
- Bazin, R., Fanchon, C., 2006. Equivalence of face and volar forearm for the testing of moisturizing and firming effect of cosmetics in hydration and biomechanical studies. *Int. J. Cosmet. Sci.* 28, 453–460.
- Benson, H.A.E., 2005. Transdermal drug delivery: penetration enhancement techniques. *Curr. Drug Deliv.* 2, 23–33.
- Betz, G., Aeppli, A., Menshutina, N., Leuenberger, H., 2005. In vivo comparison of various liposome formulations for cosmetic application. *Int. J. Pharm.* 296, 44–54.
- Bouwstra, J.A., Gooris, G.S., Bras, W., Talsma, H., 1993. Small angle X-ray scattering: possibilities and limitations in characterization of vesicles. *Chem. Phys. Lipids* 64, 83–98.
- Branco, N., Lee, I., Zhai, H., Maibach, H.I., 2005. Long-term repetitive sodium lauryl sulfate-induced irritation of the skin: an in vivo study. *Contact Dermat.* 53, 278–284.
- Coderch, L., López, O., de la Maza, A., Parra, J.L., 2002. Ceramides and skin function. *Am. J. Dermatol.* 4, 107–129.
- El Maghraby, G.M., Campbell, M., Finnin, B.C., 2005. Mechanisms of action of novel skin penetration enhancers: phospholipid versus skin lipid liposomes. *Int. J. Pharm.* 305, 90–104.
- Elsayed, M.M., Abdallah, O.Y., Naggar, V.F., Khalafallah, N.M., 2007. Lipid vesicles for skin delivery of drugs: reviewing three decades of research. *Int. J. Pharm.* 332, 1–16.
- Egelhaaf, S.U., Wehrli, E., Müller, M., Adrian, M., Schurtenberger, P., 1996. Determination of the size distribution of lecithin liposomes: a comparative study using freeze fracture, cryoelectron microscopy and dynamic light scattering. *J. Microsc.* 184, 214–228.
- Gay, C.L., Guy, R.H., Golden, G.M., Mak, V.H.W., Francoeur, M.L., 1994. Characterization of low-temperature (i.e., <65 °C) lipid transitions in human stratum corneum. *J. Invest. Dermatol.* 103, 233–239.
- Glover, K.J., Whiles, J.A., Wu, G., Yu, N., Deems, R., Struppe, J.O., Stark, R.E., Komives, E.A., Vold, R.R., 2001. Structural Evaluation of phospholipid bicelles for solution-state studies of membrane-associated biomolecules. *Biophys. J.* 81, 2163–2171.
- Holm, E.A., Wulf, H.C., Thomassen, L., Jemec, G.B.E., 2006. Instrumental assessment of atopic eczema: validation of transepidermal water loss, stratum corneum hydration, erythema, scaling, and edema. *J. Am. Acad. Dermatol.* 55, 772–780.
- Holzer, G., Riegler, E., Hönigsmann, H., Farokhnia, S., Schmidt, B., 2005. Effects and side-effects of 2% progesterone cream on the skin of peri- and postmenopausal women: results from a double-blind, vehicle-controlled, randomized study. *Br. J. Dermatol.* 153, 626–634.
- Kanikkannan, N., Singh, M., 2002. Skin permeation enhancement effect and skin irritation of saturated fatty alcohols. *Int. J. Pharm.* 248, 219–228.
- Kartono, F., Maibach, H.I., 2006. Irritants in combination with a synergistic or additive effect on the skin response: an overview of tandem irritation studies. *Contact Dermat.* 54, 303–312.
- Kim, D.-W., Park, J.-Y., Na, G.-Y., Lee, S.-J., Lee, W.-J., 2006. Correlation of clinical features and skin barrier function in adolescent and adult patients with atopic dermatitis. *Int. J. Dermatol.* 45, 698–701.
- Kim, S.D., Huh, C.H., Seo, K.I., Suh, D.H., Youn, J.L., 2002. Evaluation of skin surface hydration in Korean psoriasis patients: a possible factor influencing psoriasis. *Clin. Exp. Dermatol.* 27, 147–152.
- Koan, M.M., Blanchard, G.J., 2006. Gauging the effect of impurities on lipid bilayer phase transition temperature. *J. Phys. Chem. B* 110, 16584–16590.
- Kucerka, N., Kiselev, M.A., Balgavý, P., 2004. Determination of bilayer thickness and lipid surface area in unilamellar dimyristoylphosphatidylcholine vesicles from small-angle neutron scattering curves: a comparison of evaluation methods. *Eur. Biophys. J.* 33, 328–334.
- López, O., Cócera, M., Campos, L., de la Maza, A., Coderch, L., Parra, J.L., 2000a. Use of wide and small angle x-ray diffraction to study the modifications in the stratum corneum induced by octyl glucoside. *Colloid Surf. A* 162, 123–130.
- López, O., Cócera, M., Coderch, L., Parra, J.L., de la Maza, A., 2002. Reconstitution of liposomes inside the intercellular lipid domain of the stratum corneum. *Langmuir* 18, 7002–7008.
- López, O., Cócera, M., Walther, P., Wehrli, E., Coderch, L., Parra, J.L., de la Maza, A., 2001. Liposomes as protective agents of stratum corneum against octyl glucoside: a study based on high-resolution low-temperature scanning electron microscopy. *Micron* 32, 201–205.
- López, O., Cócera, M., Wertz, P.W., López-Iglesias, C., de la Maza, A., 2007. New arrangement of proteins and lipids in the stratum corneum cornified envelope. *Biophys. Biochem. Acta* 1768, 521–529.
- López, O., Walther, P., Cócera, M., de la Maza, A., Coderch, L., Parra, J.L., 2000b. Structural modifications in the stratum corneum by effect of different solubilizing agents: a study based on high-resolution low-temperature scanning electron microscopy. *Skin Pharmacol.* 13, 265–272.
- Marcotte, I., Auge, M., 2005. Bicycles as model membranes for solid- and solution-state NMR studies of membrane peptides and proteins. *Concept Magn. Res.* 24, 17–37.
- Miteva, M., Richter, S., Elsner, P., Fluhr, J.W., 2006. Approaches for optimizing the calibration standard of Tewameter TM 300. *Exp. Dermatol.* 15, 904–912.
- Muller-Goymann, C.C., 2004. Physicochemical characterization of colloidal drug delivery systems such as reverse micelles, vesicles, liquid crystals and nanoparticles for topical administration. *Eur. J. Pharm. Biopharm.* 58, 343–356.
- Pinnagoda, J., Tupker, R.A., Agner, T., Serup, J., 1990. Guidelines for transepidermal water loss (TEWL) measurement. A report from the Standardization Group of the European Society of Contact Dermatitis. *Contact Dermat.* 22, 164–178.
- Pinnagoda, J., Tupker, R.A., Smit, J.A., Coenraads, P.J., Nater, J.P., 1989. The intra- and inter-individual variability and reliability of transepidermal water loss measurements. *Contact Dermat.* 21, 255–259.
- Sanders, C.R., Landis, G.C., 1995. Reconstitution of membrane proteins into lipid-rich bilayered mixed micelles for NMR studies. *Biochemistry* 34, 4030–4040.
- Seok Yoon, H., Hyun Baik, S., Hwan Oh, C., 2002. Quantitative measurement of desquamation and skin elasticity in diabetic patients. *Skin Res. Tech.* 8, 250–254.
- Singh, M., Ghosh, S., Shannon, R., 1993. A direct method of beam-height correction in small-angle x-ray scattering. *J. Appl. Crystallogr.* 26, 787–794.
- Triba, M.N., Warschawski, D.E., Devaux, P.F., 2005. Reinvestigation by phosphorus NMR of lipid distribution in Bicycles. *Biophys. J.* 88, 1887–1901.
- vam Dam, L., Karlsson, G., Edwards, K., 2004. Direct observation of DMPC/DHPC aggregates under conditions relevant for biological solution NMR. *Biochim. Biophys. Acta* 1664, 241–256.
- vam Dam, L., Karlsson, G., Edwards, K., 2006. Morphology of magnetically aligning DMPC/DHPC aggregates-perforated sheets, not disks. *Langmuir* 22, 3280–3285.
- Vold, R.R., Prosser, R.S., Deese, A.J., 1997. Isotropic solutions of phospholipid bicelles: a new membrane mimetic for high-resolution NMR studies of polypeptides. *J. Biomol. NMR* 9, 329–335.
- Van den Bergh, B.A.I., Bouwstra, J.A., Junginger, H.E., Wertz, P.W., 1999. Elasticity of vesicles affects hairless mouse skin structure and permeability. *J. Controlled Rel.* 62, 367–379.
- Van der Geest, R., Elshove, D.A.R., Danhof, M., Lavnsen, A.P.M., Boddé, H.E., 1996. Non-invasive assessment of skin barrier integrity and skin irritation following iontophoretic current application in humans. *J. Controlled Rel.* 41, 205–213.

- Vold, R.R., Prosser, R.S., 1996. Magnetically oriented phospholipid bilayered micelles for structural studies of polypeptides. Does the ideal bicelle exist? *J. Magn. Reson. B* 113, 267–271.
- Whiles, J.A., Deems, R., Vold, R.R., Dennis, E.A., 2002. Bicelles in structure–function studies of membrane-associated proteins. *Bioorg. Chem.* 30, 431–442.
- Wissing, S.A., Müller, R.H., 2003. The influence of solid lipid nanoparticles on skin hydration and viscoelasticity—in vivo study. *Eur. J. Pharm. Biopharm.* 56, 67–72.
- Yilmaz, E., Borchert, H.-H., 2006. Effect of lipid-containing, positively charged nanoemulsions on skin hydration, elasticity and erythema—an in vivo study. *Int. J. Pharm.* 307, 232–238.